Optics Letters

Characterization of a carrier-envelope-offset-stabilized blue- and green-diode-pumped Ti:sapphire frequency comb

Pablo Castro-Marin,[1] Toby Mitchell,[1] Jinghua Sun,[2] and Derryck T. Reid[1,*]

[1]Scottish Universities Physics Alliance (SUPA), Institute of Photonics and Quantum Sciences, School of Engineering and Physical Sciences, Heriot–Watt University, Edinburgh EH14 4AS, UK
[2]School of Electronic Engineering and Intelligentization, Dongguan University of Technology, Dongguan, Guangdong 523808, China
*Corresponding author: D.T.Reid@hw.ac.uk

Received 30 August 2019; revised 26 September 2019; accepted 26 September 2019; posted 27 September 2019 (Doc. ID 376612); published 24 October 2019

Diode-pumping of Ti:sapphire provides a low-cost route to high-quality frequency-comb sources, exploiting the potential of direct diode modulation for wideband control of the carrier-envelope-offset frequency. We present here an f_{REP}- and f_{CEO}-locked, directly diode-pumped Ti:sapphire frequency comb, producing 66-fs pulses at 800 nm and employing f-to-$2f$ interferometry and current modulation of a 462-nm blue laser diode to achieve a stabilization bandwidth extending to ~70 kHz. Characterizations of the f_{REP} and f_{CEO} phase noise are compared to relative intensity noise spectra of the pump diodes to provide insights into how the diode design and performance transfer into the comb stability, suggesting a lower contribution to f_{REP} and f_{CEO} noise from the blue laser diode than from the green diode.

https://doi.org/10.1364/OL.44.005270

Since the original demonstration of direct diode pumping of a cw Ti:sapphire laser [1], several embodiments of modelocked diode-pumped Ti:sapphire oscillators [2] have been reported with sub-15-fs pulses [3–6], average powers exceeding 450 mW [7,8], energies of 5 nJ [8,9], single-diode pumping [4,5,9,10], wavelength-multiplexed pumping [11], and wavelength tunability across 120 nm [12]. The pump diodes employed in these systems were fabricated in the materials GaN, InGaN, or AlInGaN and operated at 445–455 nm [1–3,8,12,13], 460–480 nm [4,5,11], and around 520 nm [7,9–11]. To date, the only example of a diode-pumped Ti:sapphire laser with carrier-envelope-offset (CEO) frequency stabilization was reported in 2017 [14] and achieved CEO control by current modulating a 520-nm pump diode with a bandwidth of 55 kHz. Since this result, the InGaN laser diodes providing the highest power and highest efficiency operate in the blue 450–460 nm region [15], surpassing the performance of equivalent 520-nm green diodes and at a substantially lower cost of around $10/watt in single-unit quantities. This situation now makes blue laser diodes an attractive pump source for simple diode-based Ti:sapphire systems, with their superior price-performance ratio more than compensating for their 10–15% higher quantum defect when pumping Ti:sapphire [16]. Despite their evident advantages, blue-laser-diode pumping has until now remained unevaluated in the demanding context of femtosecond laser frequency combs. Their unique material, modal, electrical, and thermal characteristics mean that different noise performance should be expected when compared to green laser diodes. In this Letter we present—to our knowledge—the first example of a Ti:sapphire incorporating CEO frequency stabilization via current modulation of its blue-diode pump laser. The system is also repetition-rate stabilized, resulting in a fully locked frequency comb, and we present phase-noise and relative-intensity noise (RIN) characterizations that provide insights into how the performance of the pump diodes translates into the stability of the laser frequency comb.

The system architecture is illustrated in Fig. 1. We employed a wavelength multiplexed pumping scheme, in which the beams from a 520-nm 1-W Nichia NDG7475 diode and a 462-nm 2-W M462 diode were reshaped using individual cylindrical telescopes then combined on a dichroic beamsplitter (DB) to form a single pump beam. The green laser diode fast-axis (slow-axis) M^2 parameter was measured to be 1.5 (6.9), and that of the blue laser was 2.1 (6.6). An aspheric lens immediately after each diode emitter produced an approximately collimated beam, which then entered a cylindrical telescope which reduced the fast-axis beam diameter so that the pump lens ($f = 35$ mm) produced a near-symmetric focal spot in the Ti:sapphire gain medium.

The Ti:sapphire crystal had a length of 4 mm and was cut as a trapezoidal prism with an aperture of 5 mm × 6 mm and a 5° wedge between the front and back faces. It had an absorption coefficient of 4.1 cm^{-1} at 532 nm and a figure-of-merit of 100, and was coated with a highly reflecting (HR) mirror on one side and an anti-reflection (AR) coating on the other. As shown

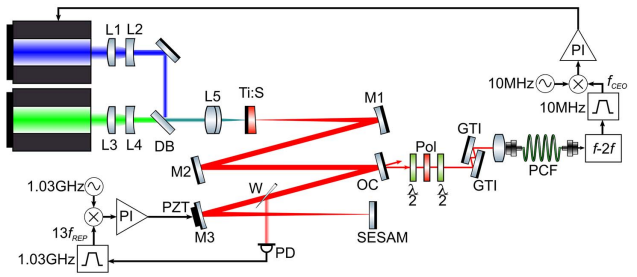

Fig. 1. Layout of the blue- and green-diode-pumped Ti:sapphire frequency comb. Cylindrical lenses L1 ($f = 150$ mm) and L2 ($f = -50$ mm) were used to reduce the diameter of the fast-axis beam from the blue laser, and lenses L3 ($f = 40$ mm) and L4 ($f = -9.7$ mm) performed the same function for the green laser. The beams were multiplexed on a dichroic beamsplitter (DB) before being focused into the Ti:sapphire crystal (Ti:S) using a doublet lens of focal length 35 mm (L5). Dispersion compensation was provided by a GTI mirror (M2), and an intracavity fused-silica 4° wedge (W) was used for coarse adjustment of f_{CEO}. Mirrors M1 and M3 were high reflectors centered at 800 nm. Other details appear in the main text.

in Fig. 1, the oscillator was configured as a linear resonator operating at a center wavelength of 800 nm, with the Ti:sapphire crystal at one end, followed by an HR mirror (M1) with a radius of 250 mm, a plane GTI mirror with a dispersion of -550 fs^2 (M2), an output coupler with 2% transmission (OC), a thin fused-silica wedge for CEO frequency (f_{CEO}) adjustment (W), an HR mirror of radius 500 mm (M3), and terminated by a semiconductor saturable absorber (Reflekron RK110B). One of the mirrors (M3) was mounted on a piezoelectric actuator (PZT) for repetition-rate control.

With both pump diodes operated at the maximum current the total incident pump power was 2.85 W and the output in modelocked operation took the form of two beams with a total power of 40 mW per beam. The beam modes were TEM00, permitting coupling with high efficiency into the photonic crystal fiber (PCF) that formed part of the f-to-$2f$ interferometer. The autocorrelation and accompanying spectrum recorded prior to entering the f-to-$2f$ interferometer (see Fig. 1) are shown in Fig. 2, along with a numerical autocorrelation inferred from the measured spectrum and implying that the pulses had full-width at half-maximum (FWHM) durations of 66 fs and transform-limited durations of 54 fs. The pulse repetition frequency (f_{REP}) was 79.23 MHz.

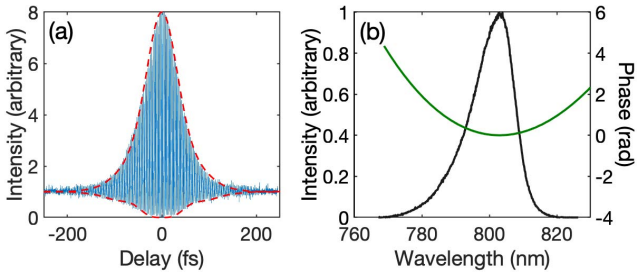

Fig. 2. (a) Autocorrelation and (b) corresponding spectrum. The best-fit autocorrelation envelope [red, (a)] was calculated by adding a quadratic spectral phase to the measured spectrum [green, (b)] to find the best agreement with the experimental measurement.

In most previously reported Ti:sapphire frequency combs f_{CEO} is stabilized by fast feedback to the power of the pump laser, commonly by using an acousto-optic modulator inserted between the pump laser and the Ti:sapphire oscillator [17]. As highlighted in [14], an attractive feature of direct diode pumping is the ability to modulate the device current with a bandwidth approaching 1 MHz, which would be sufficient to fully exploit the approximately 300-kHz modulation limit implied by the 3-μs upper-state lifetime of Ti:sapphire [18]. To access the highest modulation bandwidths we drove the pump diodes with two Wavelength Electronics LDTC2 laser diode controllers, which have a bandwidth of 1.6 MHz in constant-current mode. Figure 3(a) shows the measured open-loop diode response for a sine-wave modulation, indicating that modulation from DC to >100 kHz is possible. With closed-loop modulation the bandwidth was maintained until 350 kHz. The reason for the low-frequency rolloff is not known but we speculate that this is caused by a proprietary electrostatic protection device present in the diode package. We also investigated the RIN of each diode, and in Fig. 3(b) we present the frequency-dependent RIN relative to the carrier (left axis) along with the cumulative standard deviation of the RIN data (right axis). The measurements reveal a very low cumulative RIN of <0.001% for each device, with the largest noise contribution from a feature near 70 kHz, thought to originate from the switched-mode power supply used with the diode controller.

A common-path f-to-$2f$ interferometer [19] incorporating a 20-cm-long PCF from NKT (NL-MP-750) was used to detect f_{CEO}. Figure 4 shows the supercontinuum spectrum and

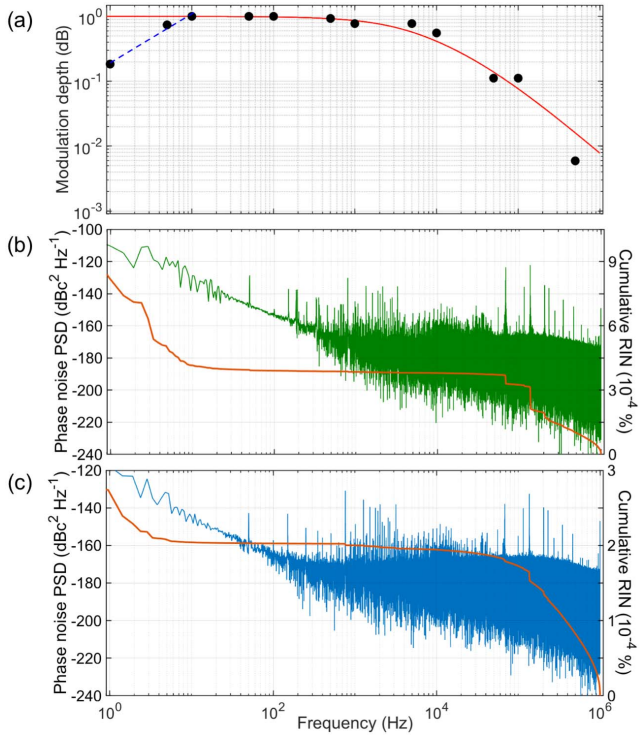

Fig. 3. (a) Blue laser diode open-loop frequency response (symbols) and fitted Bode plot (red) with three poles and three zeros. The dashed line is a fit to the low-frequency rolloff with a gradient of 7.6 dB/decade. (b) and (c) show the RIN power spectral densities and cumulative RINs integrated from 1 μs to 1 s for the green and blue laser diodes.

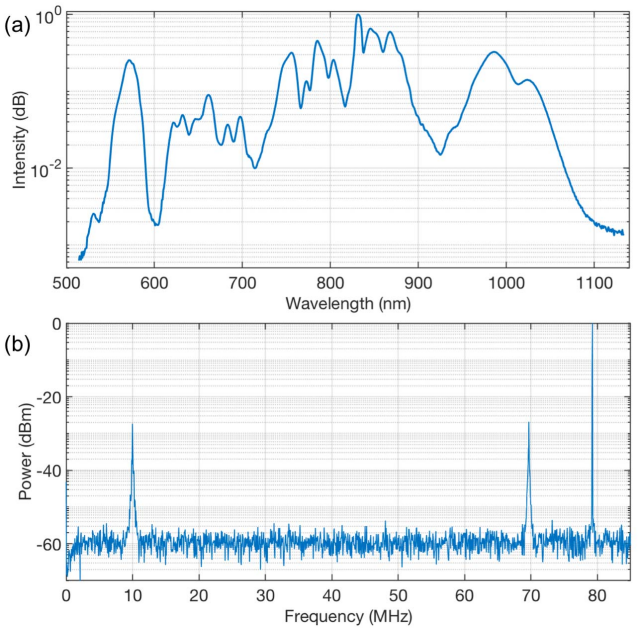

Fig. 4. (a) Supercontinuum produced by the laser and used for f-to-2f interferometry. (b) RF spectrum of the output containing the frequencies f_{CEO} (10 MHz), f_{REP}-f_{CEO} (69.2 MHz), and f_{REP} (79.2 MHz).

the radio-frequency (RF) spectrum of the output containing the frequencies f_{CEO}, f_{REP}-f_{CEO}, and f_{REP}. Typically the f_{CEO} signal exhibited a signal-to-noise ratio of around 35 dB. To stabilize f_{CEO} the detected signal was bandpass filtered at 10 MHz to isolate f_{CEO}, amplified and then converted to a digital signal using a comparator circuit.

This signal entered one channel of a 4-bit digital phase-frequency detector (PFD) [20] while the other channel received a 10-MHz reference signal. The PFD output was conditioned using a proportional-integral (PI) amplifier before being provided to the modulation input of the laser diode controller. With an appropriate choice of gain and corner frequencies f_{CEO} was stabilized across a bandwidth extending to at least 70 kHz. Figure 5 shows the power spectral density (PSD) of the in-loop error signal, showing that the cumulative phase noise integrated up to 1 MHz is 860 mrad (one-second observation time). Only 160 mrad of phase noise is accumulated between 50 Hz and 70 kHz, implying that feedback to the pump diode is effective in this frequency band. Distinct contributions are evident at 50 Hz and 70 kHz and an increasing amount above 100 kHz. This behavior can be correlated with the diode RIN and modulation characteristics given in Fig. 3; the 70-kHz diode RIN feature is weakly coupled into f_{CEO} phase noise, while the approximately 10 dB/decade high-frequency rolloff in the diode modulation characteristics above 10 kHz explains the less effective control of f_{CEO} at higher frequencies. We expect that the f_{CEO} phase noise would be significantly reduced by employing a linear power supply and better power supply line-frequency suppression. In closed-loop (as applies in f_{CEO} stabilization) the low-frequency rolloff characterized in Fig. 3(a) becomes unimportant, since the feedback signal scales to compensate. This is clear from Fig. 5, which shows no increase in phase noise from 50 Hz to the low-frequency measurement cutoff.

The f_{CEO} phase noise was recorded in-loop and can be compared to measurements from previously reported diode-pumped solid-state laser frequency combs, including a semiconductor-saturable-absorber-mirror (SESAM)-modelocked Er:glass laser [21] with an in-loop phase noise (0.1–100 MHz) of 720 mrad and a SESAM-modelocked Yb:CALGO laser [22] with an in-loop phase noise (1 Hz–1 MHz) of 680 mrad. Significantly lower phase noise was reported in a Kerr-lens-modelocked Ti:sapphire laser pumped by a frequency-doubled Nd:YVO_4 laser [23], which achieved an in-loop phase noise of 29 mrad using a more sophisticated f_{CEO} stabilization scheme. While these comparisons concentrate on in-loop measurements—and so neglect amplitude-to-phase noise originating in the PCF—they indicate an f_{CEO} stability similar to that of other directly diode-pumped solid-state laser combs, as well as promising the potential for further improvement using alternative stabilization approaches. Since a second f-to-2f interferometer was unavailable at the time of the experiment, no out-of-loop measurement was performed.

The repetition frequency was stabilized by isolating the thirteenth harmonic of 79.23-MHz repetition frequency using a microwave bandpass filter, then mixing this in an analog mixer with a 1.0299-GHz reference signal. The mixer output was conditioned in a second proportional-integral amplifier before being fed back to the PZT in the laser cavity. Figure 6 presents the power spectral density of the error signal, showing a cumulative phase noise in 13f_{REP} of 708 mrad from 1 Hz to 1 MHz, corresponding to a phase noise of 54 mrad in f_{REP}. In a similar manner to f_{CEO} locking, we observed breakthrough of the 70-kHz diode RIN in the f_{REP} phase noise. Simultaneous stabilization of f_{CEO} and f_{REP} was achieved with only minor

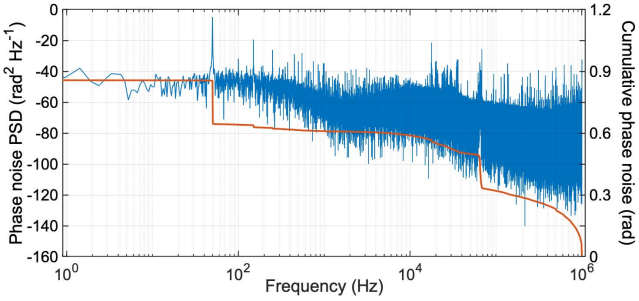

Fig. 5. In-loop measurement of the phase noise PSD and cumulative phase noise of the stabilized CEO frequency. The cumulative phase noise from 1 Hz to 1 MHz was 860 mrad.

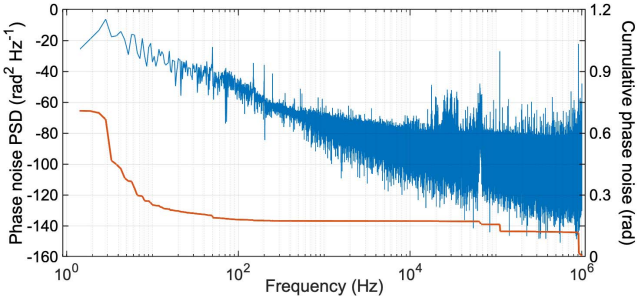

Fig. 6. In-loop measurement of the phase noise PSD and the cumulative phase noise of 13f_{REP}. The cumulative phase noise of f_{REP} from 1 Hz to 1 MHz is 54 mrad.

crosstalk observed between the locking loops, and resulting in a fully stabilized frequency comb that persisted for tens of minutes, limited by the laboratory environmental conditions.

It is useful to review the noise spectra of f_{CEO} and f_{REP} with the RIN characteristics of the blue and green laser diodes presented earlier in Fig. 3. The strongest contributions to f_{CEO} noise occur at 50 Hz (line frequency) and 70 kHz. While a 70-kHz component is present on both laser diodes, the green laser diode exhibits around an order of magnitude higher RIN at this frequency, so it may contribute to a larger extent to the f_{CEO} noise. Below 1 MHz, the greatest noise component on f_{REP} occurs around 100 kHz, which correlates with weak components present in the green and blue laser diode RIN spectra. Again, the stronger of these components is associated with the green laser. We can conclude that, while the absolute RIN of both the green and blue laser diodes is low, their noise spectra contain frequency components which correlate with f_{CEO} and f_{REP} noise. Noise on the green laser diode, which has the higher RIN, appears to couple more strongly into instabilities in f_{CEO} and f_{REP}.

In summary, we have demonstrated a fully stabilized frequency comb at 800 nm from a 66-fs Ti:sapphire laser pumped by wavelength-multiplexed 462-nm and 520-nm diode lasers. Effective stabilization of f_{CEO} across a bandwidth extending to ~70 kHz was achieved by closed-loop feedback to the current of the 462-nm laser. The cumulative phase noise from 1 Hz–1 MHz was measured to be 860 mrad for f_{CEO} and 54 mrad for f_{REP}. Power supply noise and the high-frequency modulation characteristics of the laser diode present the principal obstacles to achieving lower phase-noise performance.

Funding. Engineering and Physical Sciences Research Council (EP/N002547/1).

REFERENCES

1. P. Roth, A. Maclean, D. Burns, and A. Kemp, Opt. Lett. **34**, 3334 (2009).
2. P. Roth, A. Maclean, D. Burns, and A. Kemp, Opt. Lett. **36**, 304 (2011).
3. C. G. Durfee, T. Storz, J. Garlick, S. Hill, J. A. Squier, M. Kirchner, G. Taft, K. Shea, H. Kapteyn, M. Murnane, and S. Backus, Opt. Express **20**, 13677 (2012).
4. D. A. Kopylov, M. N. Esaulkov, I. I. Kuritsyn, A. O. Mavritskiy, B. E. Perminov, A. V. Konyashchenko, T. V. Murzina, and A. I. Maydykovskiy, Laser Phys. Lett. **15**, 45001 (2018).
5. S. Backus, M. Kirchner, C. Durfee, M. Murnane, and H. Kapteyn, Opt. Express **25**, 12469 (2017).
6. H. Liu, G. Wang, K. Yang, R. Kang, W. Tian, D. Zhang, L. Guo, J. Zhu, and Z. Wei, *Conference on Lasers and Electro-Optics*, OSA Technical Digest (Optical Society of America, 2019), paper SF3E.7.
7. K. Gürel, V. J. Wittwer, M. Hoffmann, C. J. Saraceno, S. Hakobyan, B. Resan, A. Rohrbacher, K. Weingarten, S. Schilt, and T. Südmeyer, Opt. Express **23**, 30043 (2015).
8. A. Rohrbacher, O. E. Olarte, V. Villamaina, P. Loza-Alvarez, and B. Resan, Opt. Express **25**, 10677 (2017).
9. A. Muti, A. Kocabas, and A. Sennaroglu, Laser Phys. Lett. **15**, 55302 (2018).
10. S. Sawai, A. Hosaka, H. Kawauchi, K. Hirosawa, and F. Kannari, Appl. Phys. Express **7**, 22702 (2014).
11. N. Sugiyama, H. Tanaka, and F. Kannari, Jpn. J. Appl. Phys. **57**, 52701 (2018).
12. J. C. E. Coyle, A. J. Kemp, J.-M. Hopkins, and A. A. Lagatsky, Opt. Express **26**, 6826 (2018).
13. P. W. Roth, D. Burns, and A. J. Kemp, Opt. Express **20**, 20629 (2012).
14. K. Gürel, V. J. Wittwer, S. Hakobyan, S. Schilt, and T. Südmeyer, Opt. Lett. **42**, 1035 (2017).
15. M. Murayama, Y. Nakayama, K. Yamazaki, Y. Hoshina, H. Watanabe, N. Fuutagawa, H. Kawanishi, T. Uemura, and H. Narui, Phys. Status Solidi A **215**, 1700513 (2018).
16. P. F. Moulton, J. G. Cederberg, K. T. Stevens, G. Foundos, M. Koselja, and J. Preclikova, Opt. Mater. Express **9**, 2131 (2019).
17. F. W. Helbing, G. Steinmeyer, J. Stenger, H. R. Telle, and U. Keller, Appl. Phys. B **74**, s35 (2002).
18. P. F. Moulton, J. Opt. Soc. Am. B **3**, 125 (1986).
19. V. Tsatourian, H. S. Margolis, G. Marra, D. T. Reid, and P. Gill, Opt. Lett. **35**, 1209 (2010).
20. M. Prevedelli, T. Freegarde, and T. W. Hänsch, Appl. Phys. B **60**, 241 (1995).
21. S. Schilt, N. Bucalovic, V. Dolgovskiy, C. Schori, M. C. Stumpf, G. Di Domenico, S. Pekarek, A. E. H. Oehler, T. Südmeyer, U. Keller, and P. Thomann, Opt. Express **19**, 24171 (2011).
22. S. Hakobyan, V. J. Wittwer, P. Brochard, K. Gürel, S. Schilt, A. S. Mayer, U. Keller, and T. Südmeyer, Opt. Express **25**, 20437 (2017).
23. T. J. Yu, K.-H. Hong, H.-G. Choi, J. H. Sung, I. W. Choi, D.-K. Ko, J. Lee, J. Kim, D. E. Kim, and C. H. Nam, Opt. Express **15**, 8203 (2007).